

Underwater anchored profiler Aqualog for ocean environmental monitoring

Alexander G. Ostrovskii, Andrey G. Zatsepin, Dmitry A. Shvoev, and Vladimir A. Soloviev
P.P. Shirshov Institute of Oceanology, Russian Academy of Sciences
Nakhimovsky prosp., 36, Moscow 117997, Russia
E-mail: osasha@ocean.ru

Abstract

This paper concerns with development of the ocean profiler for offshore environmental monitoring on an anchored station. The device automatically makes repeated round trips up and down a taut wire between the subsurface flotation and an anchor at the sea bottom at predefined time intervals. While profiling the water column the device conducts measurements and transmits the data to a coastal station. The oceanographic moored profiling system allows a user to obtain a regular time series of oceanographic data at a fixed geographical location by using conventional oceanographic probes, which are transported by a special carrier. A concept profiler was designed and tested during the field trials in the Black Sea and Caspian Sea in 2005-2008. The final model named Aqualog is built to carry a load of modern oceanographic instruments. It works as a lift that carries various sensors such as the FSI Excell 2" conductivity/temperature/depth probe and the Nortek Aquadopp 3D current meter. To realize the profiler's full potential, a user has an option to easily change the profiler sensors by using certain self contained probes. In field experiments, the pay load of this sea elevator also included other environmental probes e.g., dissolved oxygen sensor, fluorimeter, and turbidimeter. The programmable hardware of the profiler allowed the user to set up a robotic operation algorithm (variable movement speed, sampling frequency, and etc.). In the pilot experiments in the Black Sea a wealth of new information about the fine structure of the ocean currents and vertical stratification was obtained. These observations along with the estimates of the turbulent mixing parameters are presented and discussed.

1. Introduction

One of the goals of the national sea policy of the Russian Federation is to build new monitoring systems of the ocean natural environment. The improvement of the sea monitoring methods is essential in the context of developing the sea shelf's natural resources. The first major projects on developing oil and gas fields at the sea shelf of Sakhalin Island and the Baltic Sea gave way to special programs for industrial ecologic monitoring. Similar projects in the Russian sector of the Caspian Sea are at the phase of construction. In the agenda there are large-scale fuel/energy projects in the Arctic basin. Apart from these projects, the largest fuel oil terminals are being built at the sea ports, gas pipelines are being laid on the bottom of the sea.

The obvious negative side-effect of intensifying the industrial activity at sea is the increase of the anthropogenic stress on the marine ecosystem. In western countries there is a well-established paradigm of economic growth based on introducing ecologically clean methods of conducting economic activity at sea. These green technologies involve sufficient information coverage of the sea condition, most importantly in terms of nature safety and the disaster prevention at sea. Integrated systems of managing sea and coastal resources are being created. New technologies for collecting data on the environmental conditions are major elements of such systems. Moreover, this trend for building oceanographic devices on the junction of information technologies and sea technologies is growing quickly.

The optimal environmental monitoring systems are those that both help achieve the task of non-stop information coverage of important sea zones and their pollution, and at the same time ensure the minimization of monitoring costs. In our opinion these terms are met by remote-controlled moored oceanographic observing systems, integrated with technical means of operational data transfer. Such systems include multidisciplinary bottom mounted observatories and anchored buoy stations, equipped with special environmental sensors. From stationary

stations an underwater remote probing can be conducted, such as, for example, the acoustic Doppler current profile measurements. However to monitor ecologically significant environment parameters, contact measurements are needed in the ocean interior. Hence there arises the task of creating a moored profiling system with sensors for *in situ* measurements of temperature, conductivity, pressure, dissolved oxygen, fluorescence, turbidity and other parameters, which characterize the condition of the marine environment.

To meet this demand the project on development of a measuring instrument was initiated in 2006-2008, aimed at conducting vertical profiling of the sea waters on a moored buoy station (Ostrovskiy et al., 2008). A prototype of a sea freight lift Aquazond for oceanographic sensors was constructed: a carrier was supplied with an acoustic Doppler current meter Nortek Aquadopp 3D and conductivity probe, temperature and pressure SBE CTD 19Plus with a dissolved oxygen sensor, a fluorimeter, and a turbidity sensor. A carrier with the sensors moved up and down along the mooring line, stretched vertically between subsurface flotation and the anchor. Therefore unlike the conventional mooring where the equipment is placed on fixed depths, Aquazond allowed to make continuous measurements of vertical profiles of the marine environment characteristics. The concept profiler was tested in the Black and Caspian Seas in 2005-2008.

The research on the automatic profiling of the marine environment on a moored buoy station led us to a R&D project for creating a new observational system, called Aqualog, for real-time monitoring of the marine environment in the waters of the sea shelf and the continental slope zone. In the framework of this R&D project the equipment of the profiler Aquazond is integrated with the new technical means of data transfer in the sea interior by means of inductive modems on the subsurface flotation. The subsurface inductive modem is connected by the cable with the surface buoy, from where the data is transferred by a radio channel to a coastal receiving station. This enables the user to manage the observational process and conduct the monitoring. This article describes Aqualog - the new system for marine environmental monitoring.

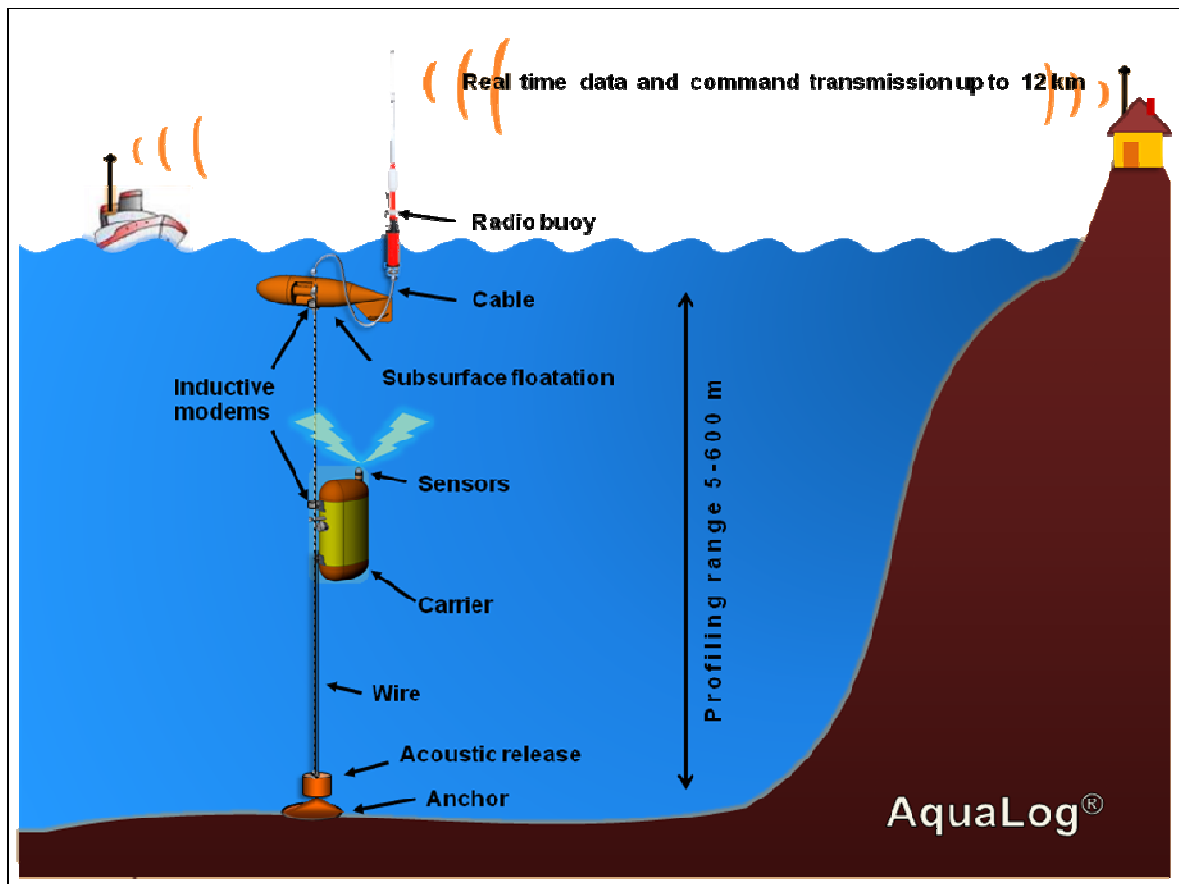


Fig. 1 The sketch of the marine environmental monitoring system Aqualog.

2. The technique

2.1 Objectives

Using the technology of water column autonomous profiling on an ocean moored station (Ostrovskiy et al., 2008) and contemporary technical means of data transfer through sea water and via air by radio, a prototype of the system for remote-controlled operational monitoring of the sea shelf and continental slope zone has been developed and produced. The sketch of the system called Aqualog is shown on Fig. 1. During a long period of time (up to one season) the system has to conduct vertical profiling, while measuring the hydrophysical and bioptical parameters of the water from the sea surface to the depth of 600 meters and providing the transfer of observational data to the coastal station for distances up to 12 km in near real-time mode.

In the first place the design of Aqualog was motivated by a necessity to conduct a monitoring of sea pollution and to forecast potentially dangerous natural phenomena. In the framework of conducting oceanographic research the Aqualog is a useful tool for field investigations of the variability of both biotic and abiotic parameters of the sea environment from a few hours to a few months. The estimation of the short-period variability and its impact on the generation of mixing is possible on the basis of regular probing during a sufficiently long time. To assess the dynamics of barotropic and baroclinic waves, eddies and wave-eddy structures and their role in the water transfer and exchange, it is necessary to observe the spatial peculiarities of hydrophysical parameters. This makes it necessary to conduct simultaneous probing by a set of Aqualogs in a number of sea locations. Finally, a topical task is revealing climate signals in the multi-year series of oceanographic data at fixed locations in sea basins and in large lakes. To achieve these objectives it is important to get regular and homogeneous ensembles of the observational data.

2.2 Approach to the coastal zone *in situ* monitoring

It is important to make the *in situ* monitoring operational. The measurements by an autonomous moored carrier have to be supplemented by exchange of data and commands with the coastal receiving station. Such a design is on the verge of two directions of ocean engineering: ocean instrumentation technology and marine information technology. It allows us to create technical means of water column operational monitoring in the coastal seas thereby making a substantial contribution into capacity building of the global ocean observation network.

The Aqualog communication pathway for data transfer between the profiling carrier and the coastal/ship receiving station consists of two main links:

- subsurface communication between the profiling probe and the surface buoy, using inductive modems,
- radio communication between surface buoy and the receiving station.

The overall data system has a number of advantages in comparison with freely floating profiling probes. Mooring has a smaller risk of loss than a freely floating buoy, allowing to conduct technical maintenance of the power source, and clean sensors from biofouling in proper time. Radio communication in the coastal zone is a budget alternative to mobile phones and satellite data transfer, as no license is required for the data exchange by radio in the band of 430-470 Hz.



Fig. 2. The Aqualog carrier. The lower photo shows the carrier without the cowl.

2.3 The Aqualog system architecture

The structure of the buoy part of the complex consists of the following equipment:

- a subsurface flotation moored with a steel wire-rope, that serves as a mooring line for a profiling carrier;
- a carrier with a number of sensors (hereafter – carrier, Fig. 2), moving along a mooring line;
- a subsurface communication system by inductive modems on the wire-rope;
- a surface buoy with modems for data and telemetry information transfer by radio;

- an acoustic anchor release.

In the carrier, the microcontroller governs a drive motor. The profiling depth and speed are controlled by the pressure sensor GE Druck PMP. The microcontroller also controls the condition of electronic equipment continuously checking electric current and voltage. On the chip 45 Savvy128 micro controller board there are the following devices: the Atmel AVR ATmega128 microcontroller itself, the slot for flash-memory of MMC-type and SD-type, a real-time clock, two RS-232 ports. A peripheral board contains the ADC Analog Device AD7708, a multiplexer for sharing serial RS-232 interface by several signals from the sensors, a fully protected dual high side switch motor drive circuit IR3220S, and the voltage converters. Analog inputs are digitized by the 16-bit resolution AD7708. The deployment set up is planned with the help of the user's computer. The following are among the profiling set up parameters:

- starting time,
- upper and lower depths with intermediate locations for stops,
- duration of the stops,
- speed of vertical movement.

The microcontroller module controls the operation of the custom sensors in the following way: the temperature, conductivity and pressure probe FSI Exell 2" Micro CTD, the acoustic Doppler current meter Nortek Aquadopp 3D and the dissolved oxygen sensor AANDERAA Oxygen Optode 4330F. The microcontroller module collects, processes and saves data measurements in the flash-memory. As an option, up to 4 additional sensors, for example the fluorimeter и turbidimeter, can be installed.

All of the electric equipment on the carrier, including measurement instruments, receives power from the pack of D size batteries.

The microcontroller module exchanges data and telemetry information with the inductive modem. The inductive modem system provides near-realtime data transmission using a plastic-coated steel mooring wire 6 mm in diameter. The SBE Underwater Inductive Modems are set on the carrier and on the subsurface flotation. In the case of the former the cable mounting bracket is set in such a way that the steel mooring wire in the plastic insulating jacket passes freely through the inductive coupler. When the carrier stops in its upmost position the observational data is transferred from the carrier to the subsurface flotation by means of an underwater inductive link. The system provides half-duplex exchange of information.

An armored mooring cable is used for data exchange between the subsurface flotation and the surface buoy. The surface buoy is essentially a spar buoy. The buoy is equipped with the wireless modem Dataradio Integra-TR and the radio antenna Anli A-100MU. The built-in radio modem is powered by a pack of valve-regulated lead-acid batteries with a gelified electrolyte. The battery pack serves also as the main ballast weight for the spar buoy.

The data exchange between the surface buoy and the coastal station is carried out at speeds up to 19.2 kbps in the band of 430-470 Hz. There are a radio modem and antennae on the coastal station identical to the ones on the radio buoy. The coastal station features a multiplexer and data synchronization module, and also a computer. The version of a coastal module in its maximum configuration allows to connect in multiplexing mode up to 4 radio modems to one computer. Up till now the basic configuration of the coastal module allowed to connect one radio modem with an opportunity of re-addressing up to 255 radio-buoys. This means that the data can be acquired by a number of moored systems in near-realtime. The receiving server is used for preliminary processing and archiving of the Aqualog data. The graphic software of the receiving server can visualize on-line data obtained from the mooring. The coastal station can be quickly installed. If needed the radio station can be installed on the ship.

Table 1. Technical specifications of the carrier of the Aqualog system.

Profiling - speed - depth range - total profiling distance ¹	0.1-0.3 m/s 5-600 m 800 km
Maximum horizontal current velocity	1 m/s
Buoyancy up to	±20 N, (±1 N recommended)
Battery pack - lithium D-size batteries - alkaline D-size batteries	36 pcs 168 Ahr 36 pcs 60 Ahr
Voltage	9 – 13.5 VDC
Turning on/off	By magnetic switch or as preprogrammed
Indication of the status	LED on the top cowl
Custom measurements	Pressure, salinity, temperature, current velocity vector ² , dissolved oxygen, inclination, heading
Vertical resolution ³ - pressure, salinity, temperature - velocity - dissolved oxygen	0.05-0.15 m 0.6-1.8 m 0.8-2.4 m
Measurement accuracy - pressure - temperature - salinity - velocity - oxygen	0.04% of the range 0.002 °C 0.002 psu 1% of measured value ± 0.5 cm/s < 8 µM or 5%
Optional sensors	Turbidimeter, fluorimeter
Dimensions	1.2×0.35×0.55 m
Weight in air (without sensors)	62 kg

¹With lithium battery pack, in still waters

²Measurement cell position from the sensor head 0.35–1.85 m

³Depends on the profiling speed



Fig. 3 The housing for the carrier electronics including the battery pack.

2.4 Features of the system

The modern materials and parts were used to build the system as follows:

- polyacetal (polyoxymethylene) for instrument and battery pack housing and certain parts of the carrier,
- ultra high molecular weight polyethylene for the carrier frame,
- glass spheres for the buoyancy,
- direct-current drive with a magnetic shaft.

The specifications of the carrier are shown in Table 1.

All the modules of the carrier, including the sensors, are mounted on the frame, which has almost neutral buoyancy in sea water. The instrument and the battery pack housing of the carrier has a cylinder shape with a diameter of approximately 200 mm (Fig. 3).

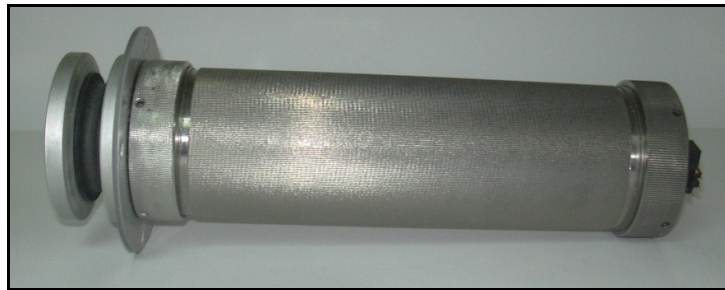


Fig. 4. The carrier's drive.

The design of the direct-current drive aims at minimizing energy consumption (Fig. 4). During stops the direct-current drive fixes the position of the carrier on the mooring line. The carrier direct-current drive features the followings:

- drive power with nominal voltage 9-13.5 V;
- gear-box;
- magnetic cylinder shaft with rare-earth magnets, inside and outside half-couplings, housing, axis, and bearings for half-couplings;
- drive-wheel with bracket, preventing the shift of the PVC coated stainless-steel wire rope;
- spring for pulling the drive wheel against the wire rope.

The motor with a gear-box and protective mechanisms runs in air inside a rigid waterproof titanium or stainless steel housing. When switching on the motor with a gear-box, the momentum is transmitted to a drive-wheel by a magnet shaft. Due to the interaction of the drive-wheel with the surface of the wire rope, the carrier begins to roll along the mooring line. The carrier moves upwards or downwards depending on the set direction for the drive-wheel's rotation.

Laboratory tests of the direct-current drive's ability to lift loads have demonstrated that a magnet shaft can lift a load weighing up to 7 kg for this drive-wheel, while when lifting heavier loads the magnet shaft slips.

In the upper and lower parts of the front part of the carrier frame's vertical plate, the leading rollers rotate to engage the mooring line and to support the carrier on the mooring line (Fig.5). The leading roller is made out of polyamide. The roller spins on a titanium axis, the ends of which are fixed to a blow-resistant housing. A special bracing was designed for the leading roller construction for simplifying the procedures of fastening and removing the carrier from the wire rope, and also for limiting possible shifts from the mooring line.

Numerical hydrodynamic modeling of the flow separation zones around the carrier was conducted while designing the geometrical shape of the carrier's cowl. Calculations were made using CAD/CAE-software SolidWorks and FloWorks for identifying the hydrodynamic drag coefficients and analyzing the peculiarities of the flow around the carrier. The numerical model

grid consisted of approximately 500 000 finite volumes. The stationary homogeneous flow was the boundary condition. The inflow horizontal speed was set at 0 m/s for the first experiment and 0.5 m/s for the second one, the speed of the carrier's vertical movement was set between 0.1 and 0.3 m/s. The inclination of the carrier equaled to 0-5°. The surface roughness of the carrier was taken as 3 µm. The experiments allowed to select the optimal shape for the carrier cowl, which would provide rather low hydrodynamic drag coefficients. In the given conditions with the battery pack nominal energy capacity of 168 Ahr, the carrier's overall profiling distance lies in the range of 200-800 km depending on the sea current speed.

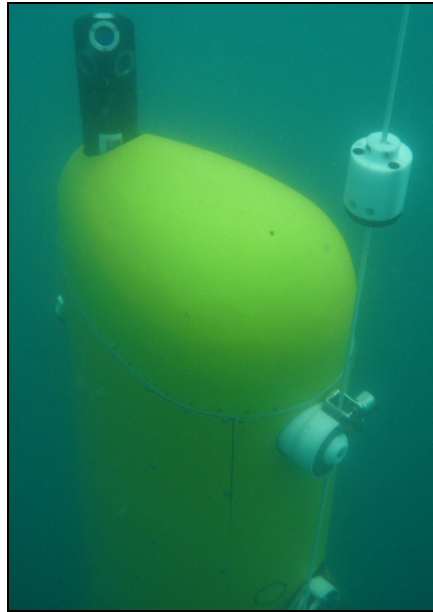


Fig. 5. The carrier in the Black sea waters. The carrier is photographed from above under a movement limiter at a depth of approximately 7 m right before another downward/upward profiling cycle. The vertically stretched mooring line is passed through the driver-wheel on the carrier. In the upper left part of the carrier an acoustic Doppler current meter Nortek Aquadopp 3D is shown.

The custom measurement instruments are high-precision, stable and fast-response. When the carrier is moving with the speed of 0.1 m/s the vertical profiles are measured with a vertical resolution of 0.05 m for pressure, conductivity and temperature (FSI Exell 2'' Micro CTD), 0.6 m for the current speed (Nortek Aquadopp 3D) and 0.8 m for the dissolved oxygen (AANDERAA Oxygen Optode 4330F).

The radio buoy is shown in Fig.6. The radio buoy specification is shown on table 2.

Table 2. Technical specifications of the radio-buoy of the Aqualog system.

Radio frequency	430-470 MHz
Highest baud rate	19.2 Kbps
Battery capacity for receive operation	1000 hrs
Battery capacity for transmit operation at maximum RF output power of 5 Watts	40 hrs
Dimensions	4.5×1.3×0.35 m



Fig. 6. The Aqualog radio-buoy.

3. Using the Aqualog for studies of the Black Sea

The processes of turbulent mixing in the Black Sea deserve special attention due to a need to study the redox zone and the anaerobic environment. The causes for weak vertical exchange in this largest meromictic basin are well-known. However a short-period mesoscale variability of turbulent mixing is not explored well enough and systematic measurements of the vertical exchange, unfortunately, have not been made.

In addition, to the absence of strong persistent currents in the Black Sea interior, tides in the inertial band are meant. The Black Sea Rim Current tends to flow round obstacles of the bottom topography. Over the continental slope and the shelf, an enhancement of the vertical mixing is anticipated, because turbulence is generated as a result of impact of the underwater troughs and canyons on near-bottom flows. The slope gravity currents of the inertial band are developed in the canyons, whereas the effects of the bottom roughness influence the dynamic processes, especially internal waves. The cross-shelf motions, for example, in the meanders of the Rim Current or in the submesoscale or mesoscale eddies in the shelf zone and the continental slope zone, can also lead to the generation of internal waves and, as a consequence, to the appearance of turbulence in stratified waters.

In July 2007, the Aqualog system was deployed to investigate short-term variability of the turbulent exchange in the waters over the continental slope off the Gelendzhik Bay (44°30'-44°35' N) in the north-eastern Black Sea. The profiling was carried out from the near-surface layer down to the near-bottom layer. During the survey, the weather was calm and warm, a seasonal thermocline was well developed; no intensive wind mixing or free convection event was noted. The background conditions favored observations of turbulent mixing.

From the 11th to the 13th of July 2007 44 profiling cycles were conducted. The Aqualog carrier with oceanographic sensors moved up and down along the wire rope between the depth of 9 m and 242 m. The profiler ran with 1 hour interval. The downward profiling speed was equal to 0,18-0,19 m/s. The ascent was faster, with a speed of 0.21 m/s, i.e. to move from the near-bottom layer to the subsurface layer it took approximately 18 minutes.

The hydrophysical measurements were carried out only during the upward legs of the profiling cycles. The sampling rate of temperature, pressure and salinity was 2 Hz. The period of averaging the current meter data was 5 s, the interval between the ensembles of the current data was equal to 1 s. Therefore, 44 sets of the vertical profiles of the hydrophysical parameters were obtained.

The intensity of the vertical mixing can be estimated from vertical profiles of density and current velocity having the fine structure resolution at the scales of 1 m, by using parameterization for the coefficient of vertical exchange (see, for example, Howard et al. 2004, Samodurov 2005). Such parameterizations are based on two approaches: those, involving the Richardson number, Ri (e.g., Pacanowski and Philander 1981), and others, implying the energy flux towards small scales along the wave-frequency spectrum of the internal waves (Gregg 1989, Wijesekera et al. 1993, Samodurov 2005). It is worth mentioning that the parameterizations of Ri via the coefficients of vertical eddy viscosity K_m and eddy diffusivity K_v are broadly used in numerical models of ocean circulation.

The estimates of the Richardson number Ri are applied when analyzing the conditions favorable for developing the shear instability. The linear theory of stratified fluids predicts the development of the shear instability when Ri is less than the critical value equaling $Ri = 0.25$. The value $Ri < 1$ indicates that there is a possibility of flow instability (Orlanski and Bryan 1969).

The gradient Richardson number is given by the following formula:

$$Ri = N^2 / |\Delta U / \Delta z|^2 \quad (1)$$

where $N^2 = g/\rho_0 (\Delta\sigma_\theta/\Delta z)$ is the buoyancy frequency and $U(z) = u(z)i + v(z)j$ is the horizontal component of the current velocity, ΔU denotes difference of the velocity values between adjacent depth bins having thickness Δz . The mean gradient Richardson number is calculated by the following formula (e.g., Howard et al. 2004)

$$\langle Ri \rangle = \langle N^2 \rangle / \langle U_z^2 \rangle \quad (2)$$

where the angle brackets denote averaging in time and depth such as

$$\langle U_z \rangle = (\langle \Delta u / \Delta z \rangle, \langle \Delta v / \Delta z \rangle). \quad (3)$$

The scale of space and time averaging has to be taken into account when interpreting the estimate $\langle Ri \rangle$. The average gradient Richardson number is to be considered as a measure of probability of the shear instability, which can be found on scales much smaller than the scales of the averaging.

For calculating the mean gradient Richardson number according to the results of the experiment in the Black Sea on July 11-13, 2007, the period of 6 s was chosen, during which the carrier moved by approximately 1.7 meter. The vertical scale of averaging the profiles is bigger

by factor of 3 than the smallest necessary for improving the correlation of signal/sound of the conductivity sensors (usually 2 s in conditions typical for the upper layer of the Black Sea). Also, the averaging corresponding to the vertical step of 1.7 m sufficiently resolves the fine structure of the sea waters.

To assess the intensity of the vertical turbulent exchange usually we used the semi-empirical formulas that relate the coefficients of vertical turbulent exchange to the observed hydrophysical parameters (Pacanowski and Philander 1981) as follows

$$K_m = A_0/(1+aRi)^n + A_1, K_v = K_m/(1 + aRi) + A_2. \quad (4)$$

The following values for constants were suggested in (Pacanowski and Philander 1981)

$$A_0 = 5 \cdot 10^{-3} \text{ M}^2/\text{c}; A_1 = 10^{-4} \text{ M}^2/\text{c}; A_2 = 10^{-5} \text{ M}^2/\text{c}; a = 5; n = 2. \quad (5)$$

The equations (4-5) are used to assess the vertical exchange from the *in situ* data of the ocean fine structure (e.g., Muench et al. 2002, Howard et al. 2004).

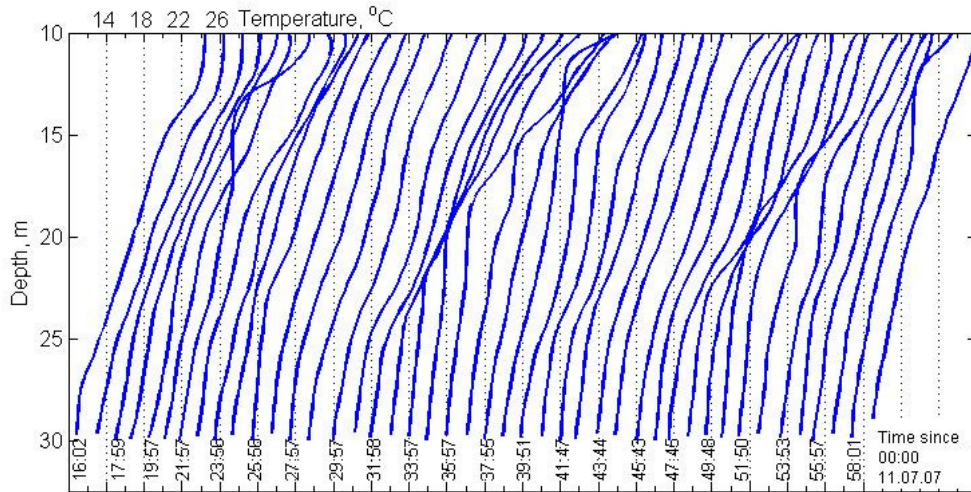


Fig. 7. The sequence of vertical profiles of the sea temperature obtained by the Aqualog system in the upper layer of the Black Sea at the mooring station off the Gelendzhik Bay on July 11-13, 2007. Only top parts (10 m - 30 m) of the deep profiles are shown to emphasize the variability in the thermocline. For visualization purposes, the profiles are shifted relative to each other by 2°C along the time axis.

The thermocline was located between the depths of 10 m and 30 m (Fig. 7). Across the thermocline, the temperature dropped from almost 23°C to 12°C. The temperature gradient varied in time, periodically sharpening; the maximum value of $\Delta T/\Delta z \sim 2^\circ\text{C}/\text{m}$ was observed 3 times during the survey as follows: in the first case early at night at 11:15 pm on July 11 in the depth range 12-14 meters, in the second case after midday July 12 2:11 pm at 10-12 meters depth, and in the third case in the morning July 13 10:19 am also at 10-12 meters. Obviously, these events were not phase locked with the regular daily cooling cycle at the sea surface. In the second and the third cases there was a quick rise of the thermocline lower boundary from 23-25 meters to 10-12 meters. The time interval between the events of sharpening the gradient was 16-20 hours.

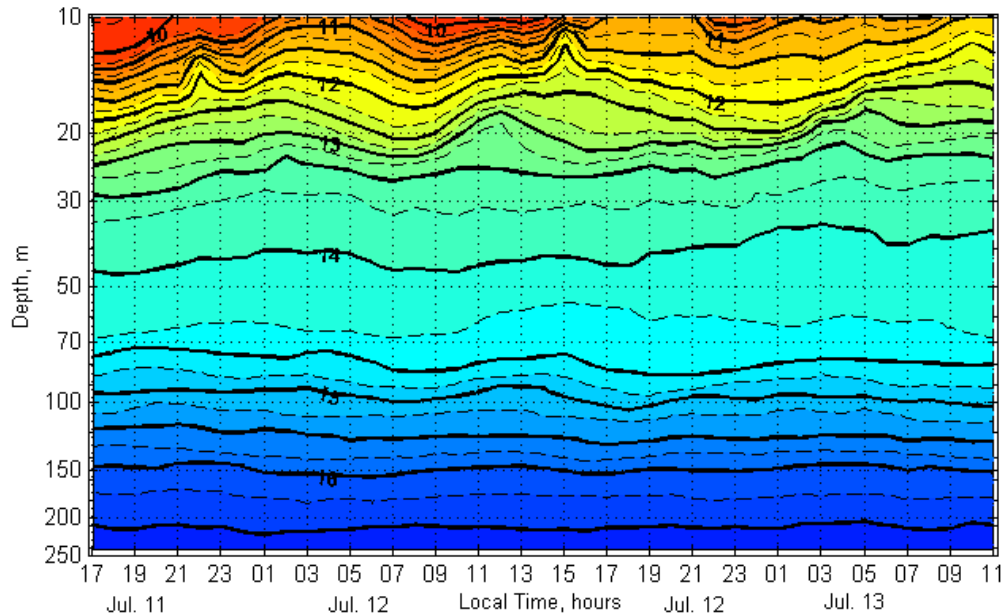


Fig. 8 The vertical distribution of σ_t (kg/m^3) observed by means of the profiling at the mooring station off the Gelendzhik Bay in the Black Sea. To visualization variability in the subsurface layer, the depth on the vertical axis is shown in the logarithmical scale.

In Fig.8, variations of isopycnals σ_t during the same observational survey, as the vertical profiles on Fig. 7, are shown. The data of σ_t were linearly interpolated on regular time-depth grid. In Fig. 8 easily seen are vertical fluctuations of the pycnocline with the period of 17-19 hours. Particularly interesting are the events of rapid rise of the isopycnal $\sigma_t = 12 \text{ kg/m}^3$ at the depths 10-15 meters around 10:00 pm on July 11 and around 3:00 pm on July 12. It is interesting that in both cases in about 2 hours after these events there was a rise of isopycnals in the near-surface layer. The isopycnal $\sigma_t = 11 \text{ kg/m}^3$ remained elevated during 3-4 hours. The gradual rise of isopycnals near the sea surface was also observed in the early morning of July 13 with a delay of 3-4 hours after the rise of the isopycnals at the depths of 20-25 meters. In the morning of July 13, the upper mixed layer became shallowest. The inertial oscillations led to periodic shoaling of the upper mixed layer.

Measurements carried out by the acoustic Doppler current meter Nortek Aquadopp3D, mounted on the Aqualog carrier, revealed a complex structure of the sea current field (Fig. 9). The inertial flow dominated in the upper 30-meter layer. The direction of the flow changed with period of 16-18 hours in accord with inertial cycle at the latitude of the survey. The current between 15 and 30 meters depth was opposite to that in the upper portion of the pycnocline and in the near-surface layer. The amplitude of the inertial current was stronger in the along-coast direction; the maximum current speed of about 0.2 m/s was observed in the near-surface layer when the current was directed south-eastward.

If typical speed of the inertial flow is 0.1 m/s then the diameter of the inertial motion is 1.9 km i.e., the horizontal dimension of inertial gyre is comparable with the width of the sea shelf in this region. When moving into the shelf the cross-shelf inertial flow in the lower layer tends to push the pycnocline up while in the opposite phase of the inertial cycle when the cross-shelf flow is directed offshore the pycnocline moves downward in the shelf waters. The analysis of Fig. 8 in conjunction with Fig. 9 shows that the change of the current direction from westward to eastward in the subsurface layer between 20 and 30 meters depth led to elevation of the pycnocline. Therefore inertial current not only contributed to the water exchange in the cross-shelf direction but also modified the horizontal pressure gradient in the outer shelf waters.

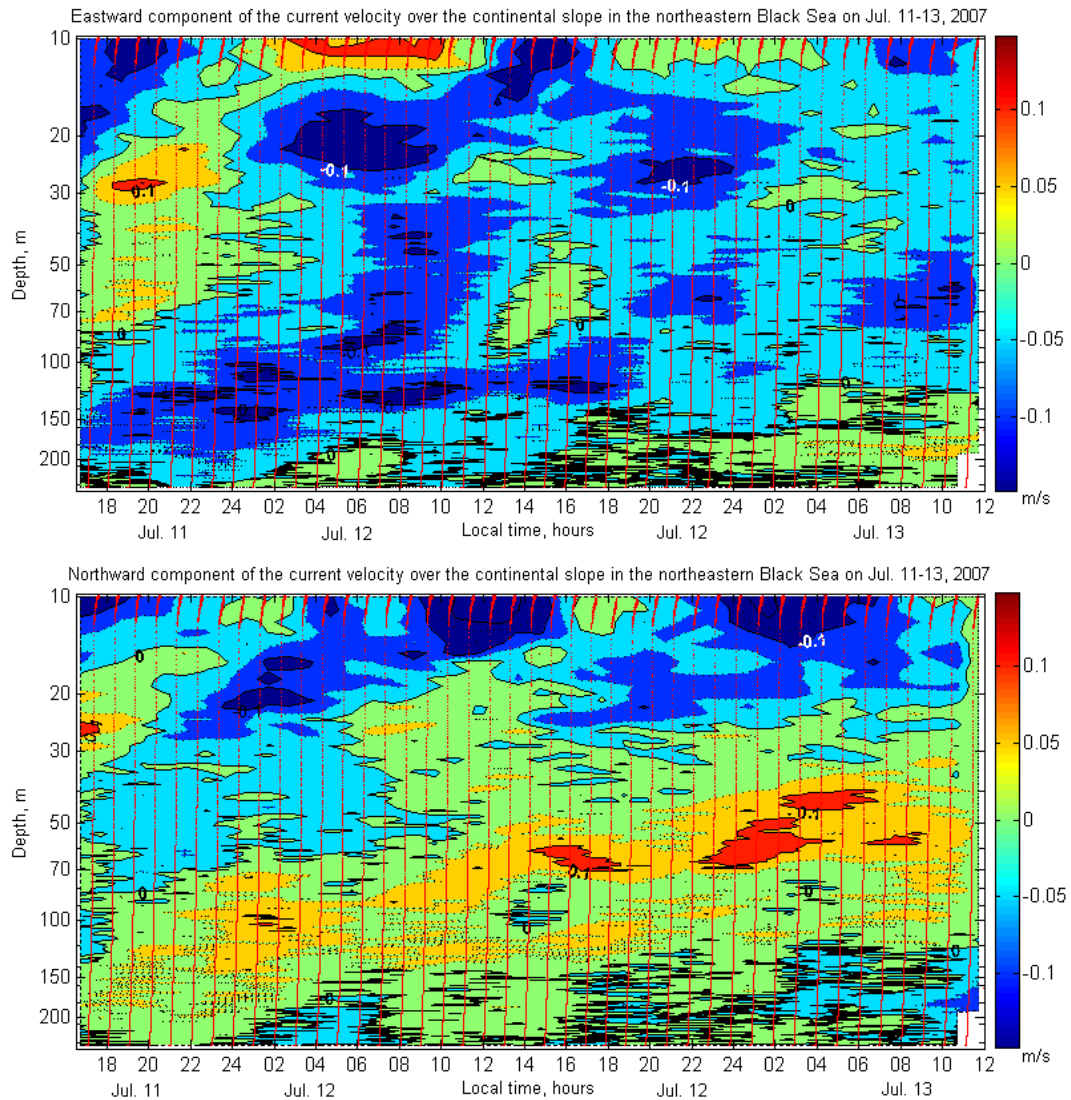


Fig. 9. The time-depth plot of the horizontal components of the current velocity obtained during the Aqualog survey at the mooring station off the Gelendzhik Bay in the Black Sea. The upper plot shows eastward current, the lower plot shows northward current. Red dots indicate location of the Aqualog carrier at upward profiling legs during the survey.

The north-westward flow was observed both above and inside the main pycnocline at the intermediate depths. During the survey, the core of northward flow, having speed of 0.05 - 0.07 m/s, moved upward from the depth of 70-180 meters to the depth of 30-120 meters. This process was accompanied by the strengthening of the south-eastward countercurrent in the deep layer below the main pycnocline. In the upper part of the main pycnocline immediately below the core of the northward jet at the depths of 70-90 meters there was a shear layer. The current shear zone at its bottom was conditioned by the sharp slowdown of the northward flow. The southward motions with speed of 0.01 m/s occurred at the depth 80-110 meters twice during the survey as follows: from 12:00 to 16:00 of July 12 and from 01:00 to 05:00 of July 13. Such motions were localized in the layer up to 30-meter thick. Below this layer the northward flow extended till the upper boundary of the deep south-eastward countercurrent.

The occurrence of the reverse motions in the core of the main pycnocline is remarkable on its own right. The shear current zone might indicate the near-inertial internal waves. Yet it is unclear whether the internal wave could reach 30-40 meters in amplitude when it approached the continental slope of the Black Sea. Notice that such vertical scale of the shear zone due to

inertial motions in the lower portion of the pycnocline was observed, for example, over the slope of the Antarctic Peninsula (Howard et al. 2004).

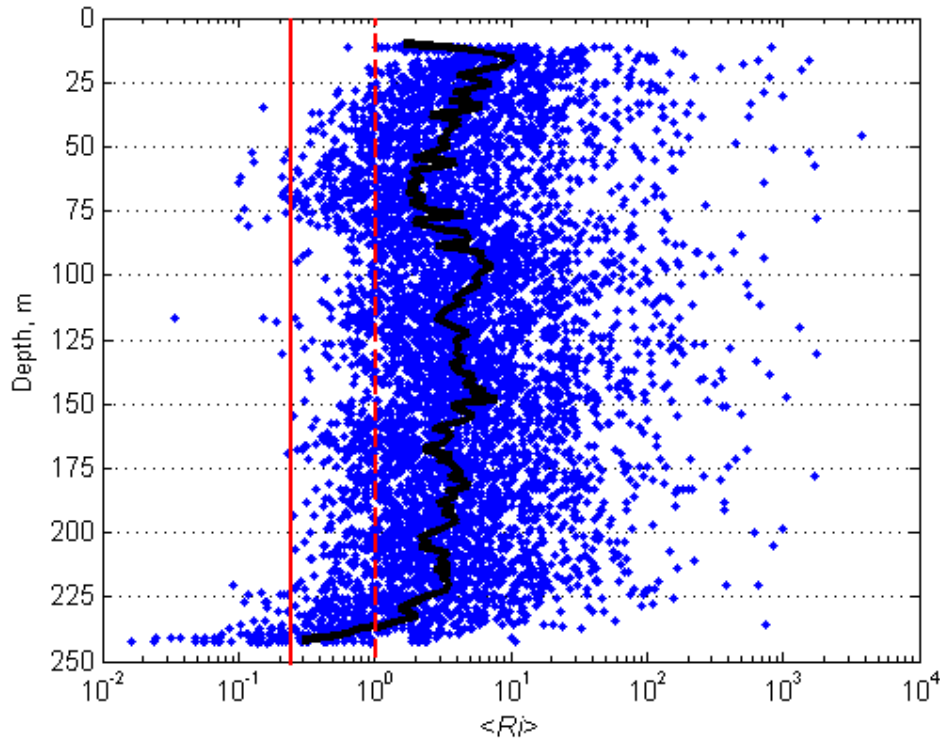


Fig. 10. The mean gradient Richardson number $\langle Ri \rangle$ (blue dots) as estimated from the Aqualog profiling data at the mooring station off the Gelendzhik Bay in the Black Sea on July 11-13, 2007. The thick black line is the vertical profile of the median values $\langle Ri \rangle$. Red line indicates $\langle Ri \rangle = 0.25$. Red dotted line indicates $\langle Ri \rangle = 1$.

Whatever was the cause of the intermittent reverse motion below the core of the north-westward flow, the current shear might lead to generation of turbulence if N was smaller than the value U_z by factor of 2 (1). The estimates of the Richardson number $\langle Ri \rangle$ (3) reveal that the patches of the turbulence could appear at the depth of 50-80 m where $\langle Ri \rangle$ was sometimes less than the threshold value of 0.25.

The estimates $\langle Ri \rangle$ computed from 44 vertical profiles of the observational data are shown in Fig. 10. Also Fig. 10 demonstrates the vertical profile of the median values of 2-m binned estimates $\langle Ri \rangle$. The profile of the median values has local minimum in the layer between 50 meters and 75 meters whereas several dozen estimates $\langle Ri \rangle$ did not exceed 1. The other region of turbulent mixing was located in the 25-meter thick near-bottom layer, which is in agreement with conventional view on interaction between sea dynamics and bottom topography. The upper mixed layer where the low values of $\langle Ri \rangle$ were anticipated was rather shallow and was located mostly above the upper depth of the profiling.

The analysis has shown that the conditions favorable for the shear instability in the sea layer between 50 meters and 80 meters appeared in the second half of the survey after the northward jet moved upward. The eddy viscosity K_m and the eddy diffusivity K_v (4) was calculated from the estimates of the mean gradient Richardson number. The results of the calculations indicated that in the layer from 50 to 80 meters, the estimates K_m increased 3-4 times in the second half of the survey compared with those of at the beginning of the survey. There was a significant amount of individual K_m estimates in the range $2 \div 10 \times 10^{-4} \text{ m}^2/\text{s}$, which is several times higher than the background values above and below the main pycnocline.

4. Conclusion

The coastal systems worldwide have embarked on rapid and diverse changes, and are under anthropogenic stress. A comprehensive network of profilers is needed to interpret the trends on a local scale superimposed on the background of global climate change. The profiler Aqualog satisfies the diverse interests of researchers involved into marine environmental surveys, fishery, and maritime logistics. The anchored profiler can be commercially applied in the pollution monitoring near offshore oil and gas rigs and maritime terminals. The vertical profiles of scalar and vectorial ocean quantities at a given location are economically more feasible to obtain by a vertically moving sensor platform rather than by a large number of fixed instruments. It would be especially important for scientific research to deploy a network of profilers along the coast so as to capture the essential spatial signals.

New data concerning circulation and vertical exchange in the sea shelf waters has been obtained by using the profiler Aqualog. The pilot field experiment in the Black Sea has shown that the profiling system allows us to obtain new data on the vertical structure of the current velocity. Such profiles with the resolution of the order of 1 meter are capable to resolve narrow jets and streams in the ocean interior. The profiling at short time intervals has provided us with new information about the ocean dynamics at the inertial frequency band. Importantly, the Aqualog system output includes high accuracy vertical profiles of ocean current velocity, temperature, and salinity. While combining these data one can rather thoroughly describe the fine structure of the ocean dynamics. Such profiling data are indispensable for identifying the processes that determine vertical and horizontal exchanges.

This study was supported by the Federal Scientific Technical Research Program RP-22.1/001 “Development of the Technology of Multilevel Regionally-Adjusted Ecological and Geodynamic Monitoring of the Seas of the Russian Federation Primarily in the Regions of the Shelf and Continental Slope,” the Federal Research Program “World Ocean” (contract no. 43.634.11.007), Program 17 of the Presidium of the Russian Academy of Sciences, and the Russian Foundation for Basic Research grants 05-05-64927, 06-05-08092-ofi, 06-05-02105-e_k, 08-05-12046-ofi.

References

1. Gregg, M.C., Scaling turbulent dissipation in the thermocline: A review. *Journal of Geophysical Research*, 1989, 94, 9686-9698.
2. Howard S.L., J. Hyatt, and L. Padman, Mixing in the pycnocline over the western Antarctic Peninsula shelf during Southern Ocean GLOBEC, *Deep-Sea Research II*, 2004, 51, 1965–1979.
3. Muench, R. D., L. Padman, S. L. Howard, and E. Fahrbach, Upper ocean diapycnal mixing in the northwestern Weddell Sea, *Deep Sea Res. II*, 2002, 49, 4843-4861.
4. Orlanski, I., and K. Bryan, Formation of the thermocline step structure by large amplitude internal gravity waves, *Journal of Geophysical Research*, 1969, 74, 6975-6983.
5. Ostrovskii, A. G., A. G. Zatsepin, V. A. Derevnin, S. S. Nizov, S. G. Poyarkov, A. L. Tsybul'skiy, and D. A. Shvoev, Akvazond moored automatic measuring system for vertical profiling of the marine medium, *Oceanology*, 2008, 48, 275–283.
6. Pacanowski, R.C., and S.G.H. Philander, Parameterization of vertical mixing in numerical models of tropical oceans, *Journal of Physical Oceanography*, 1981, 11, 1443-1451.
7. Samodurov, A.S., Formation of structures, energy dissipation and vertical exchange in stratified basins, 2005, Extended abstract of Dr. Sci. Thesis, Marine Hydrophysical Institute Ukrainian Academy of Sciences, Sevastopol, Ukraine, 36 p. (in Russian).
8. Wijesekera, H., L. Padman, T. Dillon, M. Levine, C. Paulson, R. Pinkel, The application of internal-wave dissipation models to a region of strong mixing, *Journal of Physical Oceanography*, 1993, 23, 269-286.